

---

# Quantification of Regional Myocardial Blood Flow Using Dynamic H<sub>2</sub><sup>15</sup>O PET and Factor Analysis

Ji Young Ahn, Dong Soo Lee, Jae Sung Lee, Seok-Ki Kim, Gi Jeong Cheon, Jeong Seok Yeo, Seung-Ai Shin, June-Key Chung, and Myung Chul Lee

*Department of Nuclear Medicine, Seoul National University College of Medicine, Seoul; Institute of Radiation Medicine, Seoul National University Medical Research Center, Seoul; and Department of Physics, Ewha Womans University, Seoul, Korea*

---

Because the use of factor analysis has been proposed for extracting pure physiologic temporal or spatial information from dynamic nuclear medicine images, factor analysis should be capable of robustly estimating regional myocardial blood flow (rMBF) using H<sub>2</sub><sup>15</sup>O PET without additional C<sup>15</sup>O PET, which is a cumbersome procedure for patients. Therefore, we measured rMBF using time-activity curves (TACs) obtained from factor analysis of dynamic myocardial H<sub>2</sub><sup>15</sup>O PET images without the aid of C<sup>15</sup>O PET. **Methods:** H<sub>2</sub><sup>15</sup>O PET of six healthy dogs at rest and during stress was performed simultaneously with microsphere studies using <sup>85</sup>Sr, <sup>46</sup>Sc, and <sup>113</sup>Sn. We performed factor analysis in two steps after reorienting and masking the images to include only the cardiac region. The first step discriminated each factor in the spatial distribution and acquired the input functions, and the second step extracted regional-tissue TACs. Image-derived input functions obtained by factor analysis were compared with those obtained by the sampling method. rMBF calculated using a compartmental model with tissue TACs from the second step of the factor analysis was compared with rMBF measured by microsphere studies. **Results:** Factor analysis was successful for all the dynamic H<sub>2</sub><sup>15</sup>O PET images. The input functions obtained by factor analysis were nearly equal to those obtained by arterial blood sampling, except for the expected delay. The correlation between rMBF obtained by factor analysis and rMBF obtained by microsphere studies was good ( $r = 0.95$ ). The correlation between rMBF obtained by the region-of-interest method and rMBF obtained by microsphere studies was also good ( $r = 0.93$ ). **Conclusion:** rMBF can be measured robustly by factor analysis using dynamic myocardial H<sub>2</sub><sup>15</sup>O PET images without additional C<sup>15</sup>O blood-pool PET.

**Key Words:** H<sub>2</sub><sup>15</sup>O PET; factor analysis; regional myocardial blood flow

**J Nucl Med 2001; 42:782-787**

---

**B**ecause H<sub>2</sub><sup>15</sup>O is freely diffusible, it is a favorable PET tracer for the measurement of regional myocardial blood flow (rMBF). Dynamic H<sub>2</sub><sup>15</sup>O PET has been used to mea-

sure rMBF (1-4). However, additional C<sup>15</sup>O blood-pool PET has been needed to draw the region of interest (ROI) on the myocardium to supplement low-quality H<sub>2</sub><sup>15</sup>O PET images. This need has been an obstacle to the popular use of H<sub>2</sub><sup>15</sup>O myocardial PET without a gas (C<sup>15</sup>O) study. Paired H<sub>2</sub><sup>15</sup>O-C<sup>15</sup>O PET is a cumbersome procedure and has the potential risk of patient movement between the two scans. Because subtraction of C<sup>15</sup>O images from H<sub>2</sub><sup>15</sup>O images is used to draw myocardial regions, misalignment between H<sub>2</sub><sup>15</sup>O images and C<sup>15</sup>O images will result in mispositioned tissue ROIs.

Since its first introduction in nuclear medicine, factor analysis has been widely used to extract pure physiologic time-activity curves (TACs) and their factor images from dynamic nuclear images (5-9). The purpose of factor analysis is to separate a few underlying but unobservable quantities, or factors, using the covariance relationship among the observed data. By singular value decomposition, the covariance-variance matrix of the observed data can be divided into the eigenvalue and eigenvector matrices. Thus, the observed data can be represented with a few sets of eigenvalues and eigenvectors that compose the greatest proportion of the total eigenvalues and eigenvectors.

Hermansen et al. (9) acquired myocardial factor images from H<sub>2</sub><sup>15</sup>O myocardial PET using a fixed-flow model and applied the myocardial factor images to define tissue ROIs without C<sup>15</sup>O blood-pool PET. However, these authors employed a modeling approach that used the lung TAC to obtain the left and right ventricular TACs, with consideration of the time delay between the lungs and the ventricles, and the computation time was long.

In this study, we measured rMBF using two-step factor analysis with dynamic H<sub>2</sub><sup>15</sup>O PET images without an additional C<sup>15</sup>O blood-pool PET scan. The purpose of dividing the procedure into two steps was to obtain the pure regional-tissue TACs by factor analysis. In the first step of the factor analysis, we obtained the input function and the spatial information for each component (myocardium and left and right ventricles) so that we could determine the myocardial regions (septal, inferior, lateral, and anterior). In the sec-

---

Received Sep. 18, 2000; revision accepted Jan. 10, 2001.

For correspondence or reprints contact: Dong Soo Lee, MD, PhD, Department of Nuclear Medicine, Seoul National University College of Medicine, 28 Yungundong Chongnongu, Seoul 110-744, Korea.

ond step of the factor analysis, by drawing an ROI on a quarter of the myocardium, we obtained regional-tissue TACs. After validation of input function–derived factor analysis by that derived from arterial sampling, rMBF measured by factor analysis was validated by microsphere studies performed simultaneously with H<sub>2</sub><sup>15</sup>O PET.

## MATERIALS AND METHODS

### Image Acquisition and Preprocessing

Six healthy dogs were anesthetized using thiopental sodium and intubated, but self-respiration was sustained. H<sub>2</sub><sup>15</sup>O dynamic myocardial PET images were acquired with an ECAT EXACT 47 scanner (Siemens Medical Systems, Inc., Hoffman Estates, IL/CTI, Knoxville, TN). Before the scan, femoral and radial arteries were cannulated for microsphere injection and blood sampling. Two forelimb veins were reserved for H<sub>2</sub><sup>15</sup>O injection and adenosine infusion.

A transmission scan was acquired using triple <sup>67</sup>Ge rod sources. After a bolus injection of 518–666 MBq H<sub>2</sub><sup>15</sup>O, dynamic H<sub>2</sub><sup>15</sup>O PET images were acquired at rest for 4 min (5 s × 12, 10 s × 9, and 30 s × 3). Adenosine was infused at a continuous velocity (0.14 mg/kg/min) for 7 min. Three minutes after the start of the adenosine infusion, dynamic H<sub>2</sub><sup>15</sup>O PET images were acquired for 4 min while the adenosine was infused.

Transaxial images were reconstructed using a filtered back-projection method with a Shepp-Logan filter having a cutoff frequency of 0.3 cycles per pixel for 128 × 128 × 47 matrices and a pixel size of 2.5 × 2.5 × 3.3 mm. The dynamic images were reoriented to the short axis using static images already reoriented to 128 × 128 × 64 matrices and a pixel size of 2.5 × 2.5 × 2.5 mm. Twenty-four reoriented slices that included myocardium were selected and summed to become six slices to increase the signal-to-noise ratio. The resulting images were six short-axis slices with a per-slice thickness of 1 cm, which was same as the width of myocardium cut after microsphere studies.

### Microsphere Studies

Three kinds of microspheres (15 μm; Dupont, Billerica, MA)—those labeled with <sup>85</sup>Sr, those labeled with <sup>46</sup>Sc, and those labeled with <sup>113</sup>Sn—were used for the rest and stress study. The number of microspheres was approximately 2.8 × 10<sup>6</sup> per unit volume for <sup>85</sup>Sr and <sup>46</sup>Sc and 2.4 × 10<sup>6</sup> for <sup>113</sup>Sn. Thirty-seven megabecquerels of microspheres were injected into the left ventricle through a catheter that had already been inserted into the left ventricular cavity through the femoral artery. The microspheres were injected simultaneously with injection of H<sub>2</sub><sup>15</sup>O through a forelimb vein.

After the dogs were killed, the heart was extracted and ventricular blood was washed gently with normal saline. The myocardium was cut along the long axis at 1-cm intervals. Six slices were obtained. Every slice was cut into four (anterior, lateral, septal, and posterior) regions, and then each region was cut into pieces and counted (counts per gram). By comparing the tissue counts with the blood sample counts, blood flow per unit mass (gram) of tissue was calculated (10).

### Factor Analysis

The reoriented images were masked (32 × 32) to include the cardiac region using a midventricular slice. The same mask was applied to all six slices. Only the first 2 min (18 frames) of the H<sub>2</sub><sup>15</sup>O dynamic data were chosen for factor analysis. The masked

images (32 × 32 × 18 × 6) were summed to be 8 × 8 × 18 × 6 matrices to reduce statistical fluctuation. We used the factor analysis algorithm based on the methods of Di Paola et al. (11) and Barber (12). In brief, the normalized TAC from each pixel, called a *dixel*, was assumed as a linear combination of the physiologic TACs (myocardium, left and right ventricle, and the other regions). After principal component analysis with the normalized *dixels*, a few eigenvectors were obtained and a new affine space was defined from these vectors. Then, using the positive constraint, this vector space was rotated until all factors had positive values, because all factors should be the pure physiologic data.

The procedure of our factor analysis was as follows. First, all six slices were used to extract factor images for the left and right ventricles and the myocardial tissues. The left ventricular TAC was obtained as an input function. Second, ROIs were drawn on the myocardial factor images to include the whole left ventricular cavity and a quarter (anterior, lateral, septal, and posterior) of a slice of myocardial tissue. The ROIs were projected onto the dynamic image, and then the second factor analysis was performed. Because the extracted TACs by factor analysis were in normalized units, the scaling factor to recover the true scale of the TACs was calculated using factor images (5,6). The average over a threshold (70%) of the maximum value of a factor image was used as the scaling factor. Thus, the scaling factor for input function was calculated with the left ventricular factor image from the first step, and the scaling factor for tissue TAC was calculated with the tissue factor image from the second step. Multiplying the normalized TACs by the scaling factor restored the true scale of the input function and tissue TACs. The whole procedure is shown as a schematic flowchart in Figure 1.

### Comparison of Input Functions Derived from Factor Analysis and Arterial Sampling

Arterial blood was sampled continually at 5-s intervals after the start of acquisition of additional H<sub>2</sub><sup>15</sup>O PET images in five dogs. At each experiment, the calibration factor between PET scanner and well counter was measured using a cylindrical phantom. The image-derived input functions, compensated by this calibration factor (counts/min/mL), were compared with input functions by blood sampling (counts/min/mL). The areas under the curves (AUCs) of the input functions obtained by factor analysis and arterial sampling were compared.

### Calculation of rMBF by Factor Analysis and ROI Method

rMBF was calculated using the following single-compartment model (4).

$$C_t(t) = F_{MM} \times f \times C_a(t) \otimes \exp^{-(f/\lambda)t} + F_{BM} \times C_a(t),$$

where  $C_t(t)$  is the radioactivity in the myocardial ROI at time  $t$ ,  $C_a$  is the input function,  $F_{MM}$  is the tissue recovery coefficient representing partial-volume effect,  $F_{BM}$  is the spillover fraction from ventricular blood to myocardium,  $f$  is flow, and  $\lambda$  is partition coefficient. Flow, tissue recovery coefficient, and spillover fraction were estimated using a nonlinear least squares fitting method. The partition coefficient was set to 0.91 (3).

rMBF was estimated with the regional-tissue TACs by factor analysis and the conventional ROI method as follows. In the second step of the factor analysis, ROIs were drawn over four regions (anterior, posterior, septal, and lateral) on the short-axis myocardial factor images including the left ventricle to extract left

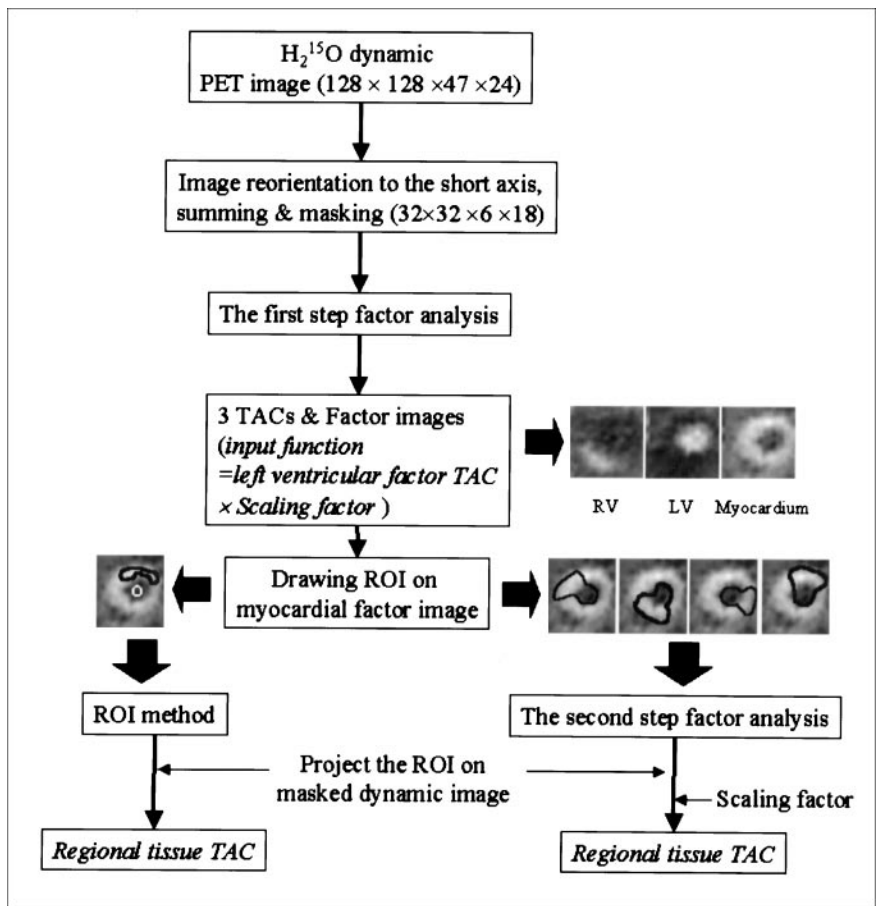


**FIGURE 1.** Schematic representation of processing steps of factor analysis to yield input function and regional myocardial TACs. LV = left ventricle; RV = right ventricle.

ventricular TAC simultaneously with tissue TACs. Tissue TACs were obtained for these four quarters of a myocardial slice and were used to estimate rMBF.

In the ROI method, tissue ROIs over the same four regions of a myocardial factor image were drawn narrowly to minimize spillover and partial-volume effects, and these ROIs were projected onto the reoriented dynamic  $H_2^{15}O$  PET images. For an input function, an ROI was drawn on the left ventricle of the midventricular level of the myocardial factor image and projected onto the reoriented dynamic  $H_2^{15}O$  PET image.

rMBFs calculated by factor analysis and the ROI method were compared with rMBF obtained by microsphere studies. All calculations, factor analyses, and rMBF estimations were performed using MATLAB (The MathWorks, Inc., Natick, MA) on an AlphaStation 600 workstation (Digital Equipment Corp., Maynard, MA).

### Data Analysis

Input functions derived from factor analysis and arterial sampling were compared with each other by calculating the relative error of AUC ( $[AUC_{\text{factor analysis}} - AUC_{\text{sampling}}]/AUC_{\text{sampling}}$ ). The correlation between rMBF by factor analysis, rMBF by the ROI method, and rMBF by microsphere studies was analyzed.

## RESULTS

### Factor Analysis

Three factor images, the result of the first step of the factor analysis, are presented in Figure 2. In all animals, the

right ventricular, left ventricular, and myocardial components were separated successfully by the first step of the factor analysis with dynamic  $H_2^{15}O$  PET images.

Image-derived input functions obtained by factor analysis were nearly the same as those obtained by arterial blood sampling except for the delay and dispersion of input by arterial sampling (Fig. 3). The mean relative error of AUC

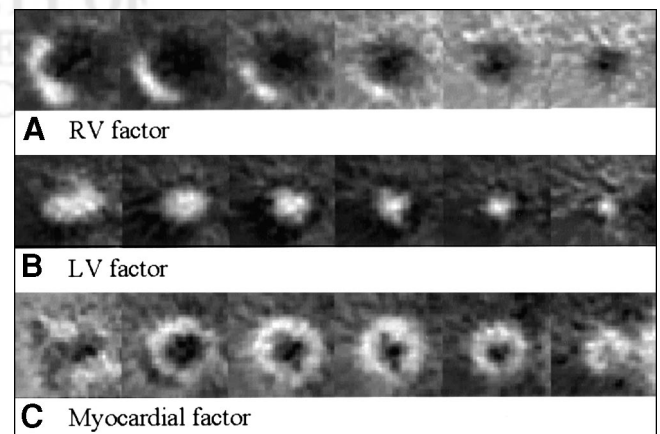


**FIGURE 2.** Right ventricular (RV) (A), left ventricular (LV) (B), and myocardial (C) factor images obtained from first step of factor analysis. All dynamic  $H_2^{15}O$  PET studies gave consistent results.

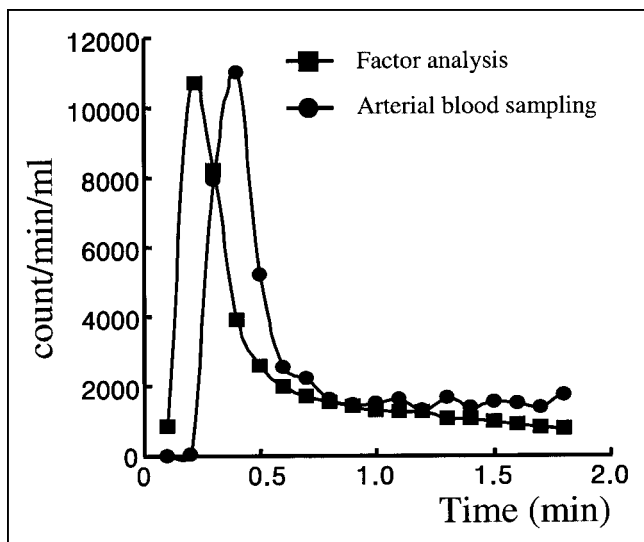


**FIGURE 3.** Input functions by factor analysis and arterial sampling. Blood samples were drawn from radial arteries.

between the curves by factor analysis and the curves by sampling was  $0.24 \pm 0.17$ .

An input function and a regional-tissue TAC obtained from factor analysis are shown in Figure 4A, and a TAC obtained from the ROI method is shown in Figure 4B. In all animals, myocardial regional-tissue TACs were extracted successfully by factor analysis.

#### rMBF Calculation and Validation

The total calculation time for the first and second steps of the factor analysis and flow estimation was  $<2$  min. The correlation between rMBF by factor analysis and rMBF by microsphere studies was good, with a correlation coefficient of 0.95 ( $P < 0.0001$ ; Fig. 5A). The correlation between rMBF by the ROI method and rMBF by microsphere studies was also good, with a correlation coefficient of 0.93 ( $P < 0.0001$ ; Fig. 5B). rMBF by the ROI method was slightly lower than rMBF by microsphere studies.

Table 1 shows the differences between the rMBF obtained by microsphere studies and the rMBFs obtained by factor analysis and the ROI method. rMBF by factor analysis tended to be higher than rMBF by microsphere studies. In the inferior wall, the difference was the largest. rMBF by the ROI method tended to be lower than rMBF by microsphere studies. The estimated spillover fraction was  $0.1 \pm 0.1$  by factor analysis and  $0.2 \pm 0.1$  by the ROI method.

#### DISCUSSION

In dynamic nuclear medicine imaging, factor analysis is now considered a powerful and robust tool to obtain pure physiologic TACs and corresponding images. Factor analysis assumes that the observed dynamic data can be represented as a linear combination of a reduced set of images, which represent most of the observed data, and their TACs. Factor analysis has been shown to have many applications

and successful results in nuclear medicine (5–9,13) and has the additional benefit of eliminating user-dependent ROI analysis (14). However, the general acceptance of factor analysis has been prevented by a negative aspect—the difficulty of interpreting the physiologic meaning of factors extracted using only the statistical characteristics of the data. The spatial and time resolutions of the nuclear medicine instruments have also limited the accuracy of factor analysis in extracting pure TACs.

The main finding of this study is that rMBF can be calculated directly from dynamic  $H_2^{15}O$  PET images through two-step factor analysis without the aid of  $C^{15}O$  blood-pool scans. Usually,  $H_2^{15}O$  PET has required an additional  $C^{15}O$  blood-pool scan to determine ROIs because of the poor quality of dynamic  $H_2^{15}O$  images. This study showed that  $C^{15}O$  scanning is no longer needed for myocardial  $H_2^{15}O$  PET. Therefore, the additional cost and radiation dose from  $C^{15}O$  scanning can be reduced by virtue of factor analysis, and the method can easily be applied to

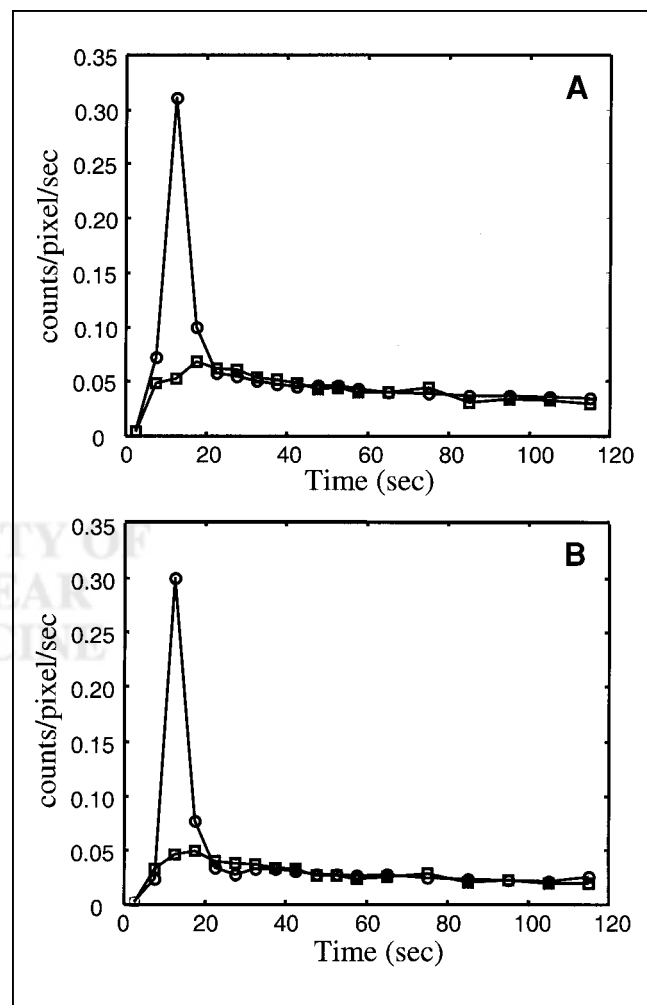


**FIGURE 4.** Representative TACs of left ventricle and myocardium. Curves were obtained by factor analysis (A) and ROI method (B).

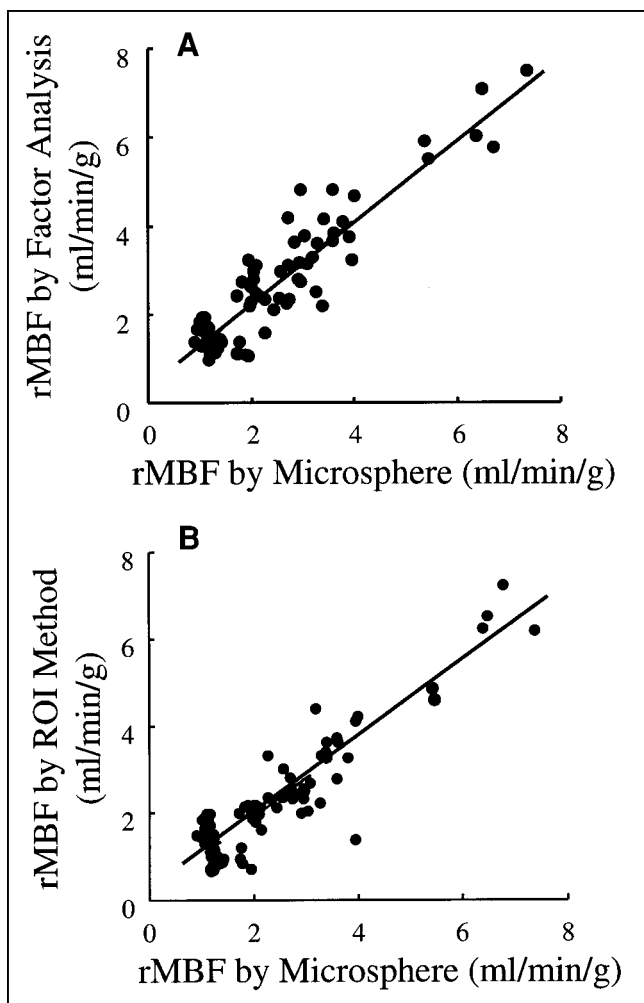


**FIGURE 5.** Correlations between rMBF by factor analysis and rMBF by microsphere studies ( $r = 0.95$ ;  $y = 0.95x + 0.26$ ) (A) and between rMBF by ROI method and rMBF by microsphere studies ( $r = 0.93$ ;  $y = 0.88x - 0.01$ ) (B).

patients undergoing  $H_2^{15}O$  PET for rMBF estimation even in PET centers without instruments for gas studies.

In the first step, we used all the slices as input data for the factor analysis; thus, three factor images (right and left ventricles and myocardium) for all slices and input function were obtained. The relative error of AUC between the input functions obtained by factor analysis and those obtained by arterial sampling was approximately 24%, mainly because

of fluctuations in the tails of the curves. The shape of both curves, however, was nearly the same except for the expected delay and dispersion of radial artery sampling. The slight difference in the tails of both curves may have been caused by counting errors in the arterial sampling. Because the shape of the initial part of the input function is mainly what affects rMBF, fluctuations in the tails of the curves are not a problem in flow estimation.

The second step of the factor analysis enabled extraction of pure regional-myocardium TACs by factor analysis without careful drawing of subtraction-defined ROIs on the myocardium (1–3). In the conventional ROI method, the regional-tissue TACs are user dependent; however, using factor analysis we could get pure regional-tissue TACs. Therefore, rMBF could be calculated robustly with the single-compartment model using the tissue TACs obtained from factor analysis. Although the estimated rMBFs obtained by factor analysis were similar to those obtained by the conventional ROI method, factor analysis is preferable to the ROI method because of the subjectivity of the latter.

Factor analysis has been applied successfully to images with a high signal-to-noise ratio (SNR), such as dynamic  $^{13}NH_3$  or  $^{18}F$ -FDG PET images (5,6). Because factor analysis for dynamic images with a low SNR was considered difficult, a modeling method was proposed for dynamic  $H_2^{15}O$  PET (9,15). In this study, we reduced statistical fluctuation by aggregating into 6 planes the 24 planes that were selected to include only the cardiac region. The pixels were also aggregated into an  $8 \times 8$  region before factor analysis was applied to the dynamic images. Moreover, in the first step of the factor analysis, the inherent difficulty of applying factor analysis to dynamic  $H_2^{15}O$  PET could be overcome using the multiplane dynamic data.

The low SNR of dynamic  $H_2^{15}O$  PET images might have influenced factor analysis, causing inaccurate oblique rotation during apex seeking (16,17). Inaccuracy in apex seeking affects the quantitative results for rMBF by using the TACs misrepresented by factor analysis. A trend was seen toward slightly higher rMBFs by factor analysis than by the ROI method and microsphere studies. This bias might have been caused by a low SNR for the dynamic  $H_2^{15}O$  PET images in the ROI chosen for the second step of the factor analysis. Contrary to the first step of the factor analysis, which used all six planes, the second step of the factor

**TABLE 1**  
Differences in rMBFs Obtained by Factor Analysis, ROI Method, and Microsphere Studies

Method	Septal	Lateral	Inferior	Anterior
Factor analysis*	$-0.07 \pm 0.44$	$-0.07 \pm 0.55$	$-0.25 \pm 0.45$	$-0.19 \pm 0.43$
ROI method†	$0.14 \pm 0.41$	$0.24 \pm 0.44$	$0.24 \pm 0.42$	$0.05 \pm 0.45$

\*Mean ( $\pm$ SD) difference between rMBF by microsphere studies and rMBF by factor analysis.

†Mean ( $\pm$ SD) difference between rMBF by microsphere studies and rMBF by ROI method.

analysis used only a quarter of a slice for extraction of the regional-tissue TAC. Although several methods have been proposed to improve the efficiency of apex seeking by overcoming this shortcoming, these methods were not applied in this study.

Spillover fraction was  $0.1 \pm 0.1$  by factor analysis and smaller ( $0.2 \pm 0.1$ ) by the ROI method, but the difference was not significant. Although we expected that use of TACs obtained from the second step of the factor analysis would remove the spillover effect from rMBF estimation, a fraction of spillover remained, indicating that our factor analysis did not perfectly separate tissue TACs from blood TACs. Nonetheless, we speculate that factor analysis was better than the subjective ROI drawing method at least for obtaining regional-tissue TACs. Further analysis is warranted to find the differences between blood-pool factor images and  $C^{15}O$  blood-pool images.

Activity was found in the lowest planes outside the myocardium. We suspect that this activity was from the liver. Although the earlier part of a TAC for liver would be different from that for myocardium because the liver is perfused mostly from the portal vein, the liver could have mimicked the TAC of myocardium. Whether similar activity would show up on human myocardial dynamic  $H_2^{15}O$  PET images is unknown. If such adjacent-organ activity were to appear, further studies would be required to exclude it.

Hermansen et al. (9) reported that the SNR of a bolus injection was higher than that of a slow infusion because the shapes of the blood and myocardium TACs differ more from each other with a bolus injection. If the tracer is infused slowly, the left ventricular and myocardial factor TACs may be less distinctive on factor analysis. If one wishes to separate the TAC of the injected  $H_2^{15}O$  in the myocardium from the TACs of radioactivity in the ventricles, rapid injection of the tracer by bolus may be better than slow infusion. In contrast, bolus injection with a high dose of  $H_2^{15}O$  may induce a dead-time effect, underestimate the input function, and thus overestimate rMBF. Therefore, injection time should be determined carefully after considering both the dead-time effect of a bolus injection and the lower probability that a slow infusion will produce clearly distinctive factor images.

## CONCLUSION

This study showed the possibility of measuring rMBF using only factor analysis of dynamic  $H_2^{15}O$  PET images, without any subtraction or modeling. Unlike the ROI method, which requires careful drawing of ROIs to mini-

mize spillover or partial-volume effects, the two-step factor analysis proposed in this study enabled robust estimation of rMBF without additional  $C^{15}O$  PET.

## ACKNOWLEDGMENTS

The authors thank Hong Jae Lee, Yong Geun Kim, and the PET center staff of Seoul National University Hospital for synthesizing the  $H_2^{15}O$  and helping with the PET studies and Sang Young Park, Myung Jin Jang, Kang Jun Seo, and Young Ae Kim for helping with the animal experiments. This study was supported by grant 04-1999-062-0 from Seoul National University Hospital and a grant from the Korea Institute of Science & Technology Evaluation and Planning.

## REFERENCES

1. Bergmann SR, Fox KA, Rand AL, et al. Quantification of regional myocardial blood flow in vivo with  $H_2^{15}O$ . *Circulation*. 1984;70:724-733.
2. Araujo LI, Lammertsma AA, Rhodes CG, et al. Noninvasive quantification of regional myocardial blood flow in coronary artery disease with oxygen-15-labeled carbon dioxide inhalation and positron emission tomography. *Circulation*. 1991;83:875-885.
3. Iida H, Kanno I, Takahashi A, et al. Measurement of absolute myocardial blood flow with  $H_2^{15}O$  and dynamic positron-emission tomography: strategy for quantification in relation to the partial-volume effect. *Circulation*. 1988;78:104-115.
4. Herrero P, Markham J, Bergmann SR. Quantitation of myocardial blood flow with  $H_2^{15}O$  and positron emission tomography: assessment and error analysis of a mathematical approach. *J Comp Assist Tomogr*. 1989;13:862-873.
5. Wu H-M, Hoh CK, Buxton DB, et al. Quantification of myocardial blood flow using dynamic nitrogen-13-ammonia PET studies and factor analysis of dynamic structures. *J Nucl Med*. 1995;36:2087-2093.
6. Wu H-M, Hoh CK, Choi Y, et al. Factor analysis for extraction of blood time-activity curves in dynamic FDG-PET studies. *J Nucl Med*. 1995;36:1714-1722.
7. Bergman H, Dworak E, Koenig B, Mostbeck A, Samal M. Improved automatic separation of renal parenchyma and pelvis in dynamic renal scintigraphy using fuzzy regions of interest. *Eur J Nucl Med*. 1999;26:837-843.
8. Samal M, Surova H, Karny M, et al. Enhancement of physiological factors in factor analysis of dynamic studies. *Eur J Nucl Med*. 1986;12:280-283.
9. Hermansen F, Ashburner J, Spinks TJ, et al. Generation of myocardial factor analysis images directly from the dynamic oxygen-15-water scan without use of an oxygen-15-carbon monoxide blood-pool scan. *J Nucl Med*. 1998;39:1696-1702.
10. Heymann MA, Payne BD, Hoffman JI, et al. Blood flow measurements with radionuclide-labeled particles. *Prog Cardiovasc Dis*. 1977;20:55-79.
11. Di Paola R, Bazin JP, Aubry F, et al. Handling of dynamic sequences in nuclear medicine. *IEEE Trans Nucl Sci*. 1982;NS29:1310-1321.
12. Barber DC. The use of principal components in the quantitative analysis of gamma camera dynamic studies. *Phys Med Biol*. 1980;25:283-292.
13. Houston AS. The effect of apex-finding errors on factor analysis to investigate the constraint problem in factor analysis and oblique transformation. *Phys Med Biol*. 1984;29:1109-1116.
14. Buvat I, Benali H, Frouin F, Bazin JP, Di Paola R. Target apex-seeking in factor analysis of medical image sequences. *Phys Med Biol*. 1993;38:123-138.
15. Hermansen F, Bloomfield PM, Ashburner J, Camici PG, Lammertsma AA. Linear dimension reduction of sequences of medical images: direct sum decomposition. *Phys Med Biol*. 1995;40:1921-1941.
16. Petras S, Aurengo A, Le D, et al. Factor analysis in successive hepatobiliary imaging of native and transplant livers. *J Nucl Med*. 1996;37:847-851.
17. Baber D, Martel A. Factor analysis revisited. *Eur J Nucl Med*. 1992;19:467-468.